

Review

Continuous Flow Synthesis of Zeolite-A from Coal Fly Ash Utilizing Microwave Irradiation with Recycled Liquid Stream

Salman Bukhari and Sohrab Rohani

Department of Chemical and Biochemical Engineering, Western University, Canada

Article history

Received: 16-12-2016

Revised: 06-06-2017

Accepted: 16-06-2017

Corresponding Author:

Salman Bukhari

Department of Chemical and Biochemical Engineering,

Western University, Canada

Tell: +1 (519) 661-2116

Email: srohani@uwo.ca

Abstract: Coal Fly Ash (CFA) was converted to zeolite using continuous microwave reactors while minimizing the wastewater produced during the zeolitization process. At bench scale, a continuous flow tubular microwave reactor was used to explore the effect of microwave irradiation on the crystallinity of the product. The waste water was reused in consecutive runs and Inductively Coupled Plasma (ICP) analysis was conducted during and after each run to observe the concentration of the cations. An increase in the production of hydroxysodalite compared to zeolite-A was noted at higher levels of microwave energy. The XRD and SEM analyses were also conducted to corroborate the results. The Cation Exchange Capacity (CEC) measurement showed the highest value of 0.405 meq/g when Deionized (DI) water was used, the CEC dropped to 0.177 meq/g for thrice recycled waste stream. It was also found that higher microwave irradiation resulted in faster crystal growth and the product crystallinity reached its maximum at 810 W of microwave irradiation in 60 min while 335 W of microwave irradiation resulted in the same crystallinity after 120 min of reaction.

Keywords: Coal Fly Ash, Synthesis, Microwave, Continuous Flow, Bench Scale, Zeolite A, Hydroxysodalite

Introduction

Despite public and private investments and advances in renewable energies, coal remains the leading source of electricity generation in the world. Currently about 40% of the global electricity is produced by coal and it is predicted to account for 33% by 2035 according to International Energy Agency (IEA, 2013) Even with this reduced share, coal will stay a major source of electricity production around the world. In 2010 alone, coal fired power plants produced about 780 million ton coal combustion products such as Coal Fly Ash (CFA) worldwide. Only about 50% of these products were recycled (Heidrich *et al.*, 2013). There has been much research conducted on producing value added products such as zeolites (Bukhari *et al.*, 2015a) from the accumulated CFA. Pioneering studies in zeolitization of CFA was reported using conventional heating (Holler and Wirsching, 1985; Shigemoto *et al.*, 1993; Hollman *et al.*, 1999), however, recently many researchers have focused their efforts on utilizing novel energy sources such as Microwave (MW) (Behin *et al.*, 2014; Bukhari *et al.*, 2014; Querol *et al.*, 1997) and

ultrasound (Bukhari *et al.*, 2016; Belviso *et al.*, 2011; Wang and Zhu, 2005; Musyoka *et al.*, 2011a).

Zeolites are crystalline aluminosilicates with a framework structure containing pores occupied by water and metallic cation. Zeolite structure is based on silicate chemistry with tetrahedron structure similar to aliphatic carbon chemistry. Silicate (SiO_4) unit within a structure is linked to other silicate through shared oxygen atoms. Zeolite frameworks exclusively contain Al^{+3} and Si^{+4} , therefore producing a negative charge in the frameworks. These frameworks contain cations to electrochemically balance the negative charge introduced by Al atoms present in aluminosilicates. Cations neutralize the excess anionic charge; and can undergo reversible ion exchange. Zeolite frameworks are also rigid which enables them to remain unaltered when water is adsorbed or desorbed.

The Si to Al ratio can range from 1 to ∞ , where the latter is complete siliceous compound, SiO_2 . The lower limit of Si to Al ratio of 1 is observed where $[\text{AlO}_4]^{-1}$ tetrahedra are not placed adjacent to each other because the negative charge on them repel each other (Breck, 1975). Some zeolites also show adsorption of anions and

organics from aqueous solution. Modification of zeolites can be achieved by several methods such as acid treatment, ion exchange and surfactant functionalization, endowing the modified zeolites higher adsorption capacity for organics and anions (Wang and Peng, 2010).

Silicate and aluminate tetrahedra are the primary building units of zeolites, whereas, the secondary building units refer to the characteristic arrangements of tetrahedra giving rise to frameworks in the zeolite's structure. The framework structures are listed in the publications of Atlas of Zeolite Framework Types which in its sixth edition lists 176 unique zeolite framework structures each assigned a 3-letter code by the commission of International Zeolite Association (Baerlocher *et al.*, 2007).

Zeolites are well known for their ability to act as catalysts, ion exchangers, adsorbents and membrane. Due to these abilities they find many potential applications in the fields of pollution control (Moreno *et al.*, 2001), radioactive waste management (Malekpour *et al.*, 2008; Sinha *et al.*, 1995), petrochemical reactions (Landau *et al.*, 2003; Babajide *et al.*, 2012), water purification (Savage and Diallo, 2005; Theron *et al.*, 2010; Shoumkova, 2011; Fan *et al.*, 2008), purification of gasses (Srinivasan and Grutzeck, 1999; Cheung and Hedin, 2014; Wdowin *et al.*, 2014) and agriculture (Khan *et al.*, 2013).

Most of the studies conducted in the field of zeolitization of CFA have utilized deionized, distilled or industrial water, however, there have been a few reports which studied other sources of water. Belviso *et al.* (2009) synthesized zeolite-X from CFA and seawater by pre-treatment fusion with

NaOH followed by hydrothermal crystallization. The synthesis yield at different crystallization temperature was higher using seawater. Hussar *et al.* (2017) synthesized zeolite-A by hydrothermal process using sodium silicate, sodium aluminate and the by-product of an aluminum etching process. Chemical composition of the aluminum etching by-product consisted mainly of oxides Al₂O₃ (92%), Na₂O (6%) and SiO₂ (0.5%). Their results indicated that higher synthesis reaction temperature and reaction time resulted in the synthesis of zeolite-A with a higher crystallinity. The effect of using industrial waste brine solution instead of ultrapure water, was investigated by Musyoka *et al.* (2011b). They used coal fly ash as silicon feedstock and high halide brine obtained from the retentate effluent of a reverse osmosis mine water treatment plant, as the solvent. The brine contained a high sodium and potassium levels and low concentrations of toxic elements. In addition, there was a trace of aluminum equal to 48.38 µg L⁻¹. The use of brine as a solvent resulted in the formation of hydroxysodalite zeolite. Musyoka *et al.* (2013) used two types of mine waters (i.e., acid and circumneutral) obtained from coal mining

operation instead of pure water to manufacture zeolites-X and zeolite-P by means of a two-step indirect (fusion followed by hydrothermal crystallization) and a direct method, respectively. The important cationic species of circumneutral water were: (Na: 952 mg L⁻¹, Mg: 38 mg L⁻¹ and Ca: 19 mg L⁻¹ and Si: 1.2 mg L⁻¹ without any Al) and acid drainage water contained: (Fe: 4694 mg L⁻¹, Na: 68 mg L⁻¹, Mg: 386 mg L⁻¹, Ca: 458 mg L⁻¹, Al: 613 mg L⁻¹ and Si: 31 mg L⁻¹). The use of circumneutral mine water resulted in similar quality zeolite-P and zeolite-X, whereas the use of acidic mine drainage led to the formation of hydroxysodalite. Behin *et al.* (2014) utilized liquid waste stream from a Plasma Electrolytic Oxidation (PEO) process. The electrolytes used in PEO typically contained low concentrations of alkaline solutions (Dehnavi *et al.*, 2013). The waste stream of PEO contained Na (673 mg L⁻¹), K (497 mg L⁻¹), Si (295 mg L⁻¹) and Al (10 mg L⁻¹) cations and the zeolite synthesized with this waste stream had a lower CEC and water carrying capacity compared to zeolite synthesized with DI water.

In addition to using waste water as mentioned above, Behin *et al.* (2016) reused and recycled the waste stream from zeolitization process. It was found that zeolite-P can be produced utilizing waste water stream.

The present work explores the utilizing of recycled waste water for the production of zeolite-A at larger scale unlike previous works focusing on the MW zeolitization of CFA at lab scale (Behin *et al.*, 2014; Bukhari *et al.*, 2014; Belviso *et al.*, 2009; Musyoka *et al.*, 2013; Behin *et al.*, 2016).

There has been some research done on a larger scale utilizing conventional heating. Moriyama *et al.* (2005) used a 0.6 L reactor for the conversion of CFA to zeolite-P at an elevated pressure of 0.48 MPa and 153°C. The liquid to solid ratio was 1.1 L kg⁻¹ in NaOH solution (3 M). The zeolite-P produced, had a CEC ranging from 1.25 to 2.0 meq/g. Querol *et al.* (2001) produced zeolite-P in a 10,000 L reactor. The reaction was conducted at 149.5°C and 0.35 MPa. The liquid to solid ratio in the slurry was 1.68 L kg⁻¹ in 2.4 M NaOH solution.

We report the work conducted in a bench MW reactor with a volume of 0.2 L.

Materials and Methods

Materials

Coal fly ash was obtained from a coal fired power plant (OPG, Nanticoke, ON, Canada) and was stored in a sealed container before use. Sodium hydroxide (Alphachem, Canada) and sodium aluminate anhydrous (Sigma-Aldrich, USA) were of analytical grade and used as received. Deionized (DI) water was used for the preparation of the solutions. Other chemicals used for characterization tests were of analytical grade.

Methods

Two sets of experiments were conducted; the first set of experiments were conducted to study the effect of MW power while the second set of experiments were to evaluate the effect of recycling the effluent stream. The schematics of the Milestone FlowSynth MW (Milestone, Italy) bench scale reactor with 1 L of reaction slurry capacity is shown in Fig. 1. There is an inner recycled stream from the FlowSynth MW reactor/crystallizer to a mixing/feed tank which is equipped with a condenser and a heating jacket for proper temperature control. The purpose of the inner recycle stream is to increase the exposure time of the slurry to the MW irradiation. The residence time of the slurry in the FlowSynth crystallizer/reactor per pass at a slurry flow rate is given in Table 1, while the overall run time was for 250 min.

MW Power Experiments

The first set of experiments, without the overall recycle stream from the MW crystallizer/reactor to the digestion tank, was carried out by adding 109 g of

sodium hydroxide granules with 91 g of fly ash (NaOH/CFA ratio of 1.2) to 850 mL deionized water and mixed/digested at 60°C for 16 h. Subsequently, 150 mL aqueous sodium aluminate solution (concentration: 0.155 g mL⁻¹) was also added in the ageing tank. The slurry with extra sodium aluminate was aged for two hours at room temperature and mixed in the mixing/feed tank attached to the MW reactor as shown in Fig. 1.

The system was kept at atmospheric pressure at 95°C with the use of a reflux condenser. The slurry was circulated through the MW reactor and samples were withdrawn from the mixing tank at predetermined times. The slurry flow was adjusted to increase the total or cumulative MW irradiation to the reaction slurry to study the effect of MW irradiation on the zeolitization process. The experimental runs with different slurry flow rates, residence times and corresponding MW power are outlined in Table 1. The block diagram of the runs without the overall recycle stream to the digestion tank is shown in Fig. 2.

Table 1. The MW power experiment sample numbers with corresponding MW power, slurry flow rates and the residence times per pass

Sample	Average MW power (W)	Flow rate (mL/min)	Residence time (s)
P-300	335	130	1.54
P-400	395	150	1.33
P-600	600	200	1.00
P-800	810	250	0.80

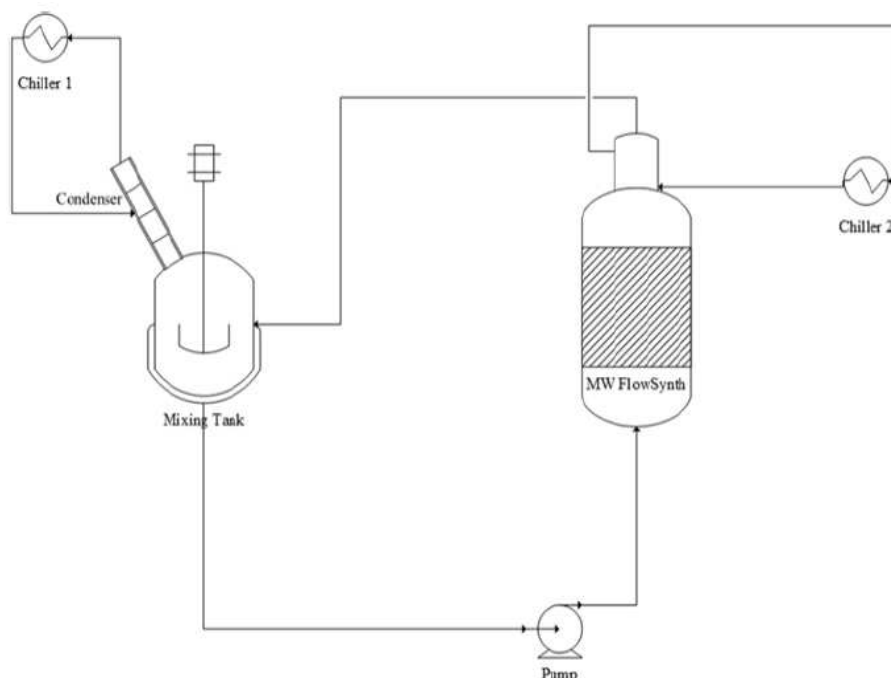


Fig. 1. The schematics of the bench scale FlowSynth MW crystallizer/reactor with an inner recycle stream to increase the exposure time to the MW irradiation

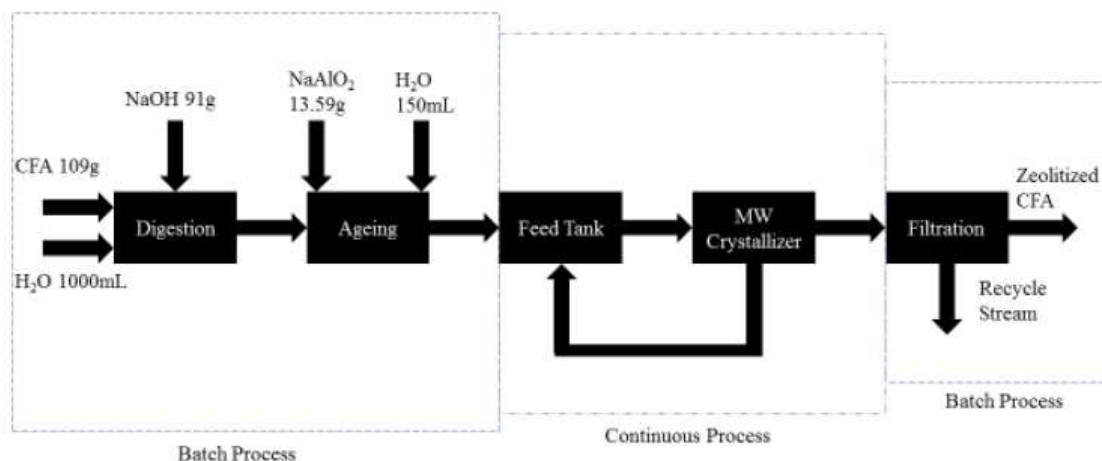


Fig. 2. The block diagram of runs without the overall recycle stream from the MW reactor/crystallizer to the digestion tank

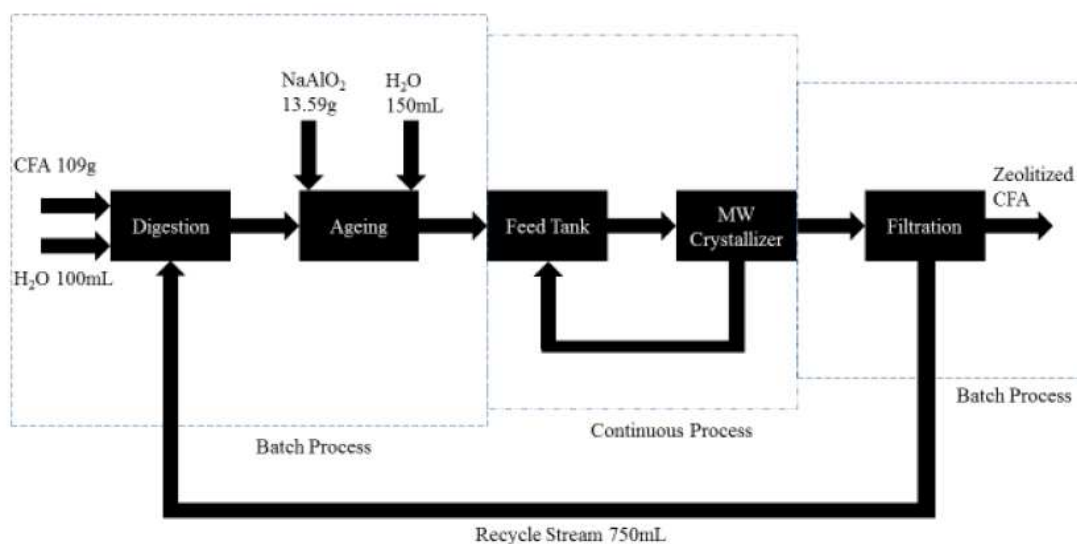


Fig. 3. The block diagram of runs with the overall recycle stream from the MW reactor/crystallizer to the digestion tank

Experiments with the Overall Recycled Stream

The slurry for the first run was prepared with DI water according to the procedure discussed above. For the successive runs with an overall recycled stream, the slurry withdrawn from the FlowSynth MW crystallizer/reactor after removing the product zeolitized CFA in the filtration system, was mixed of the DI water. Seven hundred fifty mL of the effluent stream from the FlowSynth MW reactor/crystallizer was recovered and mixed with the DI water to replenish the solvent. The loss of 250 mL of solvent in each run was associated with two major factors, some of the liquid remained in the zeolitized CFA, in addition, the liquid content inside the reactor could not be completely removed. The block diagram of the runs with the overall recycled stream is illustrated in Fig. 3.

Samples were withdrawn after each digestion and MW treatment (crystallization) to observe the metal ion concentration in the solution throughout the experiments.

Characterization

Inductively Coupled Plasma Atomic Emission Spectroscopy (ICP-AES) was used to measure the concentration of different ions in the solution both after the digestion and MW reaction. Concentrations were found using a Perkin-Elmer Optima-3300 DV ICP-Atomic Emission Spectrometer (USA). Chemical composition of the CFA sample was determined by means of X-Ray Fluorescence spectroscopy (XRF) utilizing PANalytical PW2400 Wavelength Dispersive. Rigaku-Miniflex powder diffractometer (Japan) was

used to collect XRD data of the synthesized zeolites using $\text{CuK}\alpha$ (λ for $\text{K}\alpha = 1.54059 \text{ \AA}$) over the range of $5^\circ < 2\theta < 25^\circ$ with a step width of 0.02° . The characteristic peaks of zeolitized CFA were at the 2θ of 7.20° , 10.19° , 12.49° , 16.14° and 24° (Treacy and Higgins, 2007). The peak areas were calculated using MDI-Jade v 7.5 software. The crystal size distribution and morphology of the zeolites were studied by Scanning Electron Microscope (SEM); Hitachi S 2600N SEM (Tokyo, Japan) operating at 5 kV of acceleration voltage. The Cationic Exchange Capacity (CEC) was measured using ammonium acetate saturation method (over a 5 day period) based on Bain and Smith (1987). The zeolite samples were soaked in a 1 N solution of ammonium acetate for 5 days in the same end-over-end shaker. After 5 days, the zeolite samples were filtered and allowed to air dry. The dried samples were then washed using 100 mL ($5 \times 20 \text{ mL}$) of an aqueous solution of 10 wt% NaCl and 1 vol% HCl to remove the fixated ammonium. The ammonium concentration in the supernatant was then measured. The ammonium concentration was correlated to peak absorbance intensity between 550 and 800 nm using UV-VIS spectroscopy. To prepare the samples for the UV-VIS spectroscopy, sodium salicylate, sodium hydroxide and sodium hypochlorite were added and 5 minutes allowed to elapse for the reaction to proceed to completion.

Results and Discussion

X-Ray Analysis (XRD and XRD)

The main sources of Si and Al from CFA for hydrothermal zeolitization process are summarized in Table 2. The XRD data indicated that the main components of the CFA were amorphous aluminosilicate as well as quartz and mullite that existed as crystalline structures.

The MW Power Experiments

X-Ray Diffraction Analysis (XRD)

After the digestion in the mixing tank, the feed pump was turned on at a predetermined speed indicated in Table 1 to continuously supply the CFA slurry through the MW reactor. It took the system about 10 min to reach steady state. Following steady state, samples were collected every 30 min to conduct XRD analysis. A series of characteristic peaks were observed at the 2θ of 7.25° , 10.25° , 12.55° , 16.20° , 21.80° , 24.10° , 27.25° , 30.10° and 34.35° , which were in agreement with reference peaks that belong to zeolite-A. The calculated characteristic peaks areas of the samples collected are indicated in Fig. 4.

The XRD analysis indicate that irrespective of MW power all the samples require at least 30 min before zeolitic crystals can be registered by XRD. Therefore, it indicates that the nucleation of zeolitic crystals is not a strong function of the MW power. However, once crystal growth starts, the samples irradiated under higher MW power grow faster compared to the samples irradiated with lower power. This can be concluded by observing the stronger growth of characteristic peak area of samples P-800 and P-600 which were irradiated with higher MW energy compared to samples P-400 and P-300 which were irradiated with lower MW energy. However, once the area of the characteristic peak of a sample reached a maximum, it did not increase with the increases MW power input. All samples eventually had the similar crystallinity irrespective of the MW power input level. The positive correlation between the crystal growth and microwave irradiation in zeolite-A crystallization is in agreement with earlier work (Bukhari *et al.*, 2005b).

Scanning Electron Microscope (SEM)

The SEM images of the solids were taken over the 4 h of MW irradiation. The SEM images are illustrated in Fig. 5a-e.

The SEM analysis of the MW irradiated samples show that the surface of the CFA is the nucleation and crystal growth site for the zeolites. As the reaction progresses, small cubic zeolitic-A crystals can be deciphered in the SEM images. These structures grow larger with increase in the time of MW irradiation. The SEM results corroborate with the XRD analysis which shows an increase of characteristic peak area as the MW irradiation time is increased, indicating the production of zeolite-A over the reaction period.

Table 2. XRF analysis of chemical composition of CFA

Parameter	Weight percent (%)
<i>Major oxide</i>	
SiO_2	41.78
Al_2O_3	19.61
CaO	13.64
Fe_2O_3	5.79
MgO	3.23
TiO_2	1.39
K_2O	1.10
Na_2O	0.94
P_2O_5	0.71
BaO	0.36
SrO	0.25
Cr_2O_3	0.01
MnO	0.02
<i>Loss On Ignition</i>	10.89
Total	99.72
<i>Phases analysis</i>	
Amorphous aluminosilicate	
Quartz (SiO_2)	
Mullite ($3\text{Al}_2\text{O}_3 \cdot 2\text{SiO}_2$)	

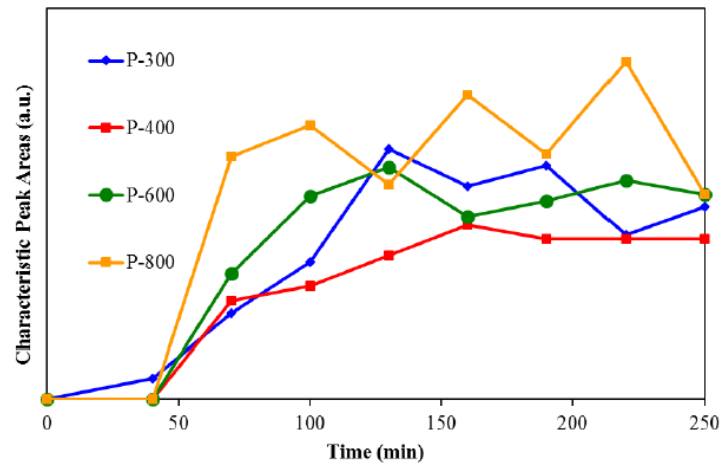


Fig. 4. XRD characteristic peak areas with respect to time

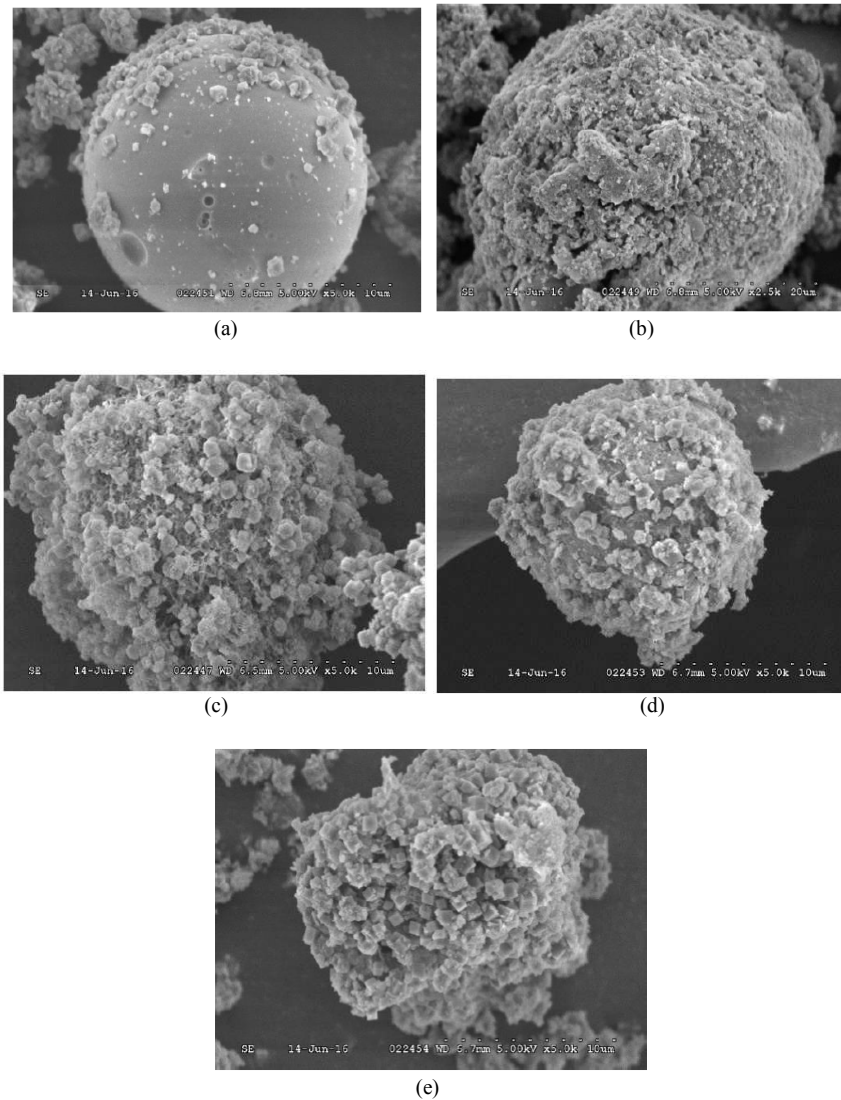


Fig. 5. SEM images of zeolitized CFA at (a) 30 min (b) 60 min (c) 90 min (d) 120 min (e) 150 min

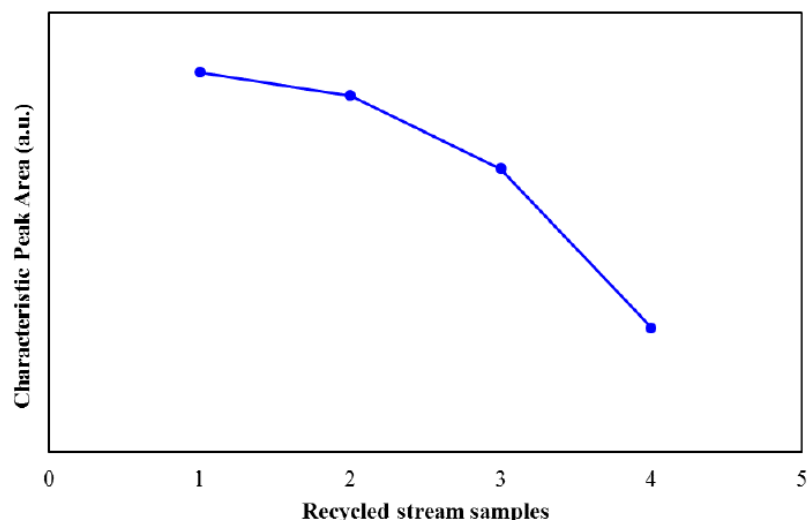


Fig. 6. The XRD characteristic peak area results for recycled stream

Recycled Stream Experiments

X-Ray Diffraction Analysis (XRD)

The XRD analyses for the recycled stream experiments were conducted after the end of each run. The characteristic peak areas are illustrated in Fig. 6.

It was observed that after each run the crystallinity of the final product was reduced, indicating that the recycling reduces the quality of zeolitic crystals compared to using fresh water. Previous works have also reported lower crystallinity (Musyoka *et al.*, 2013; Behin *et al.*, 2016) utilizing different waste streams during the zeolitization of CFA. As the recycle stream is re-used the crystallinity of the product is further decreased. This can be explained due to the increased concentration of metallic ions with consecutive runs. This observation is later corroborated with the ICP results.

Inductively Coupled Plasma Atomic Emission Spectroscopy (ICP-AES)

The ICP analysis was conducted for recycle stream experiments to track the concentration of metallic ions in the solution over the length of the whole experiment. Samples for the ICP analysis were drawn after digestion (designated by D in Fig. 7 and crystallization (designated by C in the figure).

Metallic ions including Al, As, Fe, K, Si and V were detected in the solvent. The concentration of both light and heavy metals increased with each run as indicated in Fig. 7a-c. The solid bars represent the ICP result after digestion and the shaded bars represent ICP results after digestion.

Figure 7a indicates that after digestion in the first run (D_0) both the aluminum and silicon concentration can be detected which indicates the dissolution of aluminosilicate contents of CFA in the solvent. Aluminum content is seen

to increase in each ICP sample after crystallization (C_0 to C_3) due to the addition of additional aluminum source before crystallization step. Extra aluminum is necessary for the crystallization of zeolite-A as it is observed that without extra aluminum zeolite-P is obtained (Behin *et al.*, 2016; Aldahri *et al.*, 2016).

Each ICP after crystallization shows lower concentration of Si compared to the corresponding digestion step, indicating that the Si constituents in the solution crystallize as part of zeolitic framework. It can be further noted that each consecutive digestive step results in lower concentration of Si compared to the last digestion step signifying that recycle stream is no longer able to dissolve the CFA contents compared to the fresh water. This effect becomes more significant as the liquid stream is further recycled. This could be due to the saturation of the reactant solvent with metallic ions and reducing the ionic diffusion from the CFA matrix to the solution in the digestion step.

Figure 7b and 7c show the concentration of As, Cr, K and V over the recycled stream run. It can be observed that the concentration of these metallic ions constantly increases as the recycled stream is reused.

Scanning Electron Microscope (SEM)

The SEM images of the recycled stream experiments shown in Fig. 8 were obtained for samples at the end of each 4 hour run. The images showed cubic zeolite-A and rough spherical hydroxysodalite structure. The amount of zeolitic crystals present, depended on the reactant solvent and the number of times the reactant solvent was recycled. The first two samples, one crystallized in DI water and the other in once recycled stream, had significantly higher cubic structures. However, successive experiments had fewer cubic zeolite-A structures and significantly more rough spherical hydroxysodalite

structures. The presence of various alkali metal cations in otherwise identical gels, results in the synthesis of different zeolites (Khodabandeh, 1997). The interaction between negatively charged silicate, aluminate and aluminosilicate species and the cation species is extremely

important in the crystallization of the zeolite. The presence of heavy metal cations in the solution and their interaction with the aluminosilicate can be hypothesized as one reason for the production of hydroxysodalite in the recycled stream.

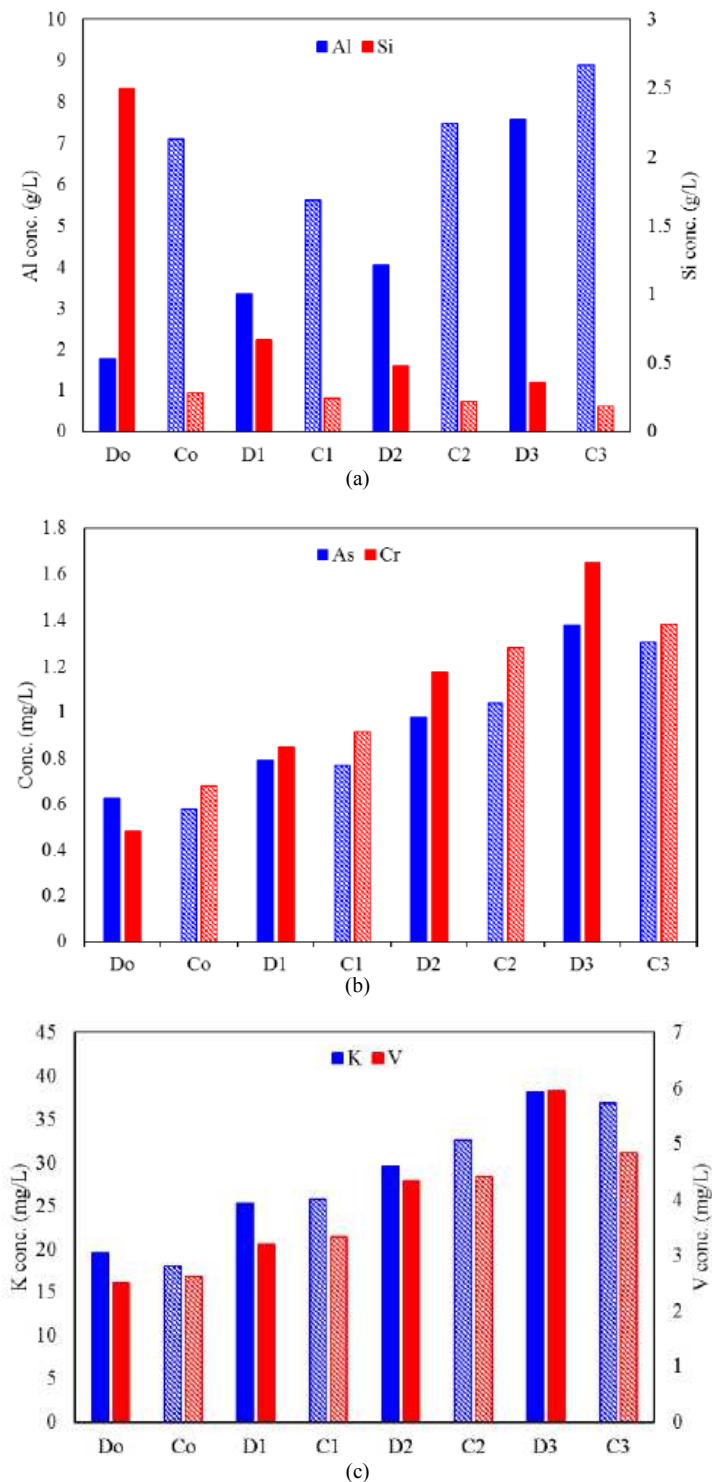


Fig. 7. ICP analysis of (a) Al, Si; (b) As, Cr and (c) K, V

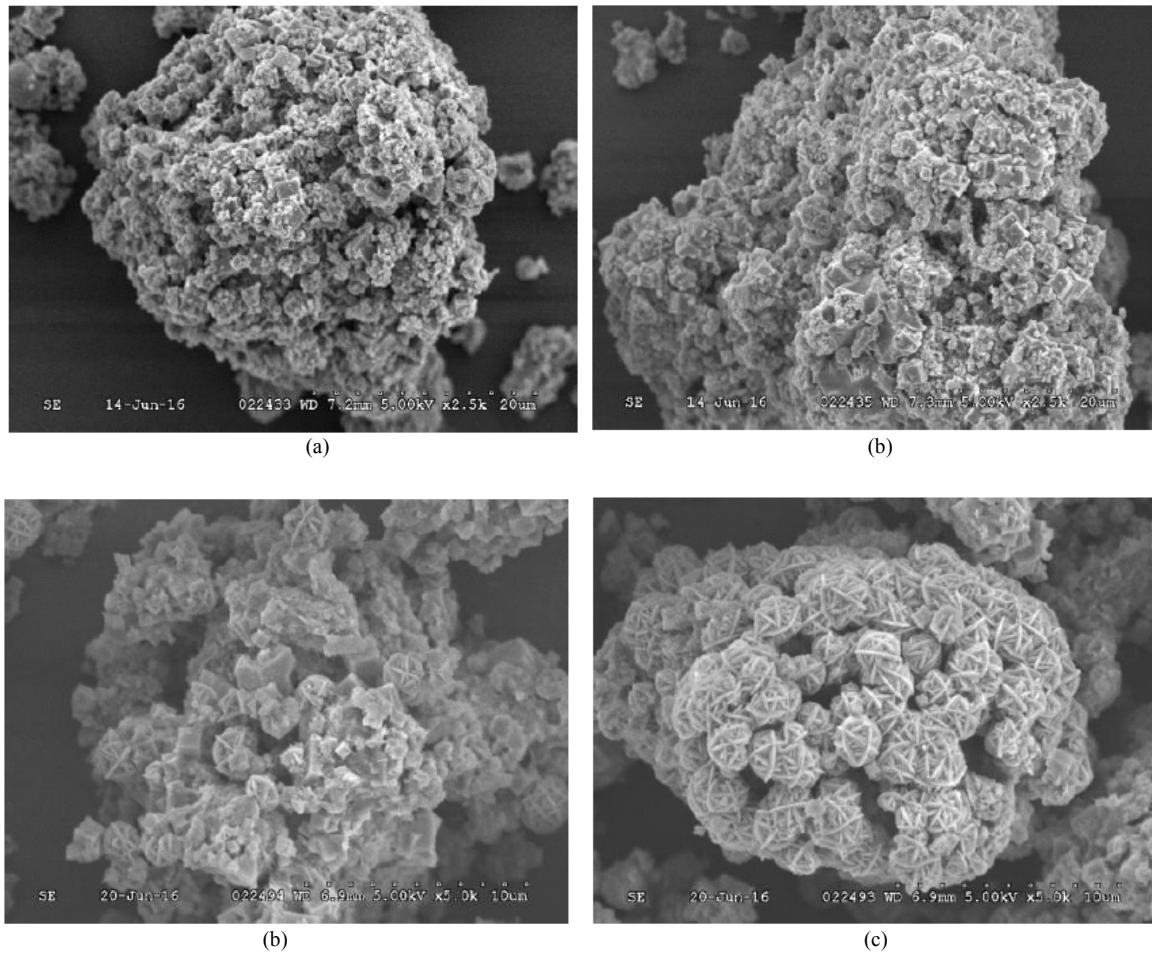


Fig. 8. SEM images of zeolitized CFA with (a) Deionized Water (b) first recycled stream (c) Second recycled stream (d) Third recycled stream

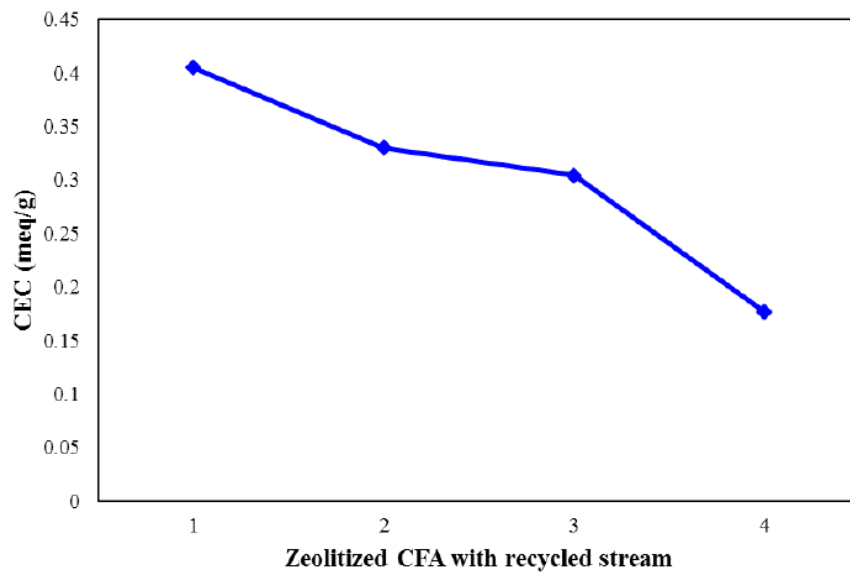


Fig. 9. CEC of zeolitized CFA with Deionized water, first recycled stream, second recycled stream, third recycled stream

Cation Exchange Capacity (CEC)

The Cation Exchange Capacity (CEC) is an important physical property of the zeolitic materials and is related to the quality of a zeolite species. Figure 9 illustrates the CEC of the zeolitized CFA synthesized with various reaction solvents.

The zeolitized CFA synthesized with DI water had the highest CEC with 0.405 meq/g and as the consecutive recycled stream was used, the resulting product had lower CEC, 0.330, 0.305 and 0.177 meq/g, respectively. A lower CEC has been previously observed when utilizing waste stream instead of pure water (Behin *et al.*, 2014; Bukhari *et al.*, 2014). The decrease in the CEC of the synthesized samples can be attributed to the higher production of hydroxysodalite. Since, hydroxysodalite has lower CEC values than zeolite A (Derkowski *et al.*, 2007).

Conclusion

Two sets of experiments converting CFA to zeolite were conducted utilizing the continuous flow MW reactor. The first set of experiment was conducted to investigate the effects of MW power on the zeolitization. It was observed that higher power of MW irradiation resulted in a faster crystal growth while after 150 min of reaction it was observed that the crystallinity reached a maximum regardless of MW power.

The first set of experiment indicates that MW power is directly correlated to the zeolite crystal growth. Higher MW irradiation power results in faster crystal growth, however, the MW irradiation does not affect the nucleation rate neither does it increase the overall conversion. This result can be used to optimize the MW power irradiation and reaction time for the zeolitization process of CFA in larger scales.

The second set of experiment was conducted with recycled waste liquid stream. The ICP analysis was conducted after digestion and after crystallization for each run. The concentration of silicon and aluminum significantly increased after each digestion step and decreased after crystallization. This signifies the dissolution of aluminosilicate constituents of CFA. The subsequent decrease of silicon and aluminum concentration in the slurry was due to the crystallizing of zeolitic crystals on the surface of CFA particles. However, each consecutive recycled stream showed lower amount of aluminosilicate. This indicates that the waste stream produced by the zeolitization process cannot be recycled indefinitely. This is also observed through XRD and SEM analysis. The XRD analysis indicated that the crystallinity of the zeolite produced with successive recycled streams was lower while the SEM showed a higher production of hydroxysodalite compared to zeolite-A. The CEC analysis further

indicated that the zeolite produced with DI water had higher CEC of 0.405 meq/g compared to the runs with the recycled streams of 0.330, 0.305 and 0.177 meq/g. The decreased in the CEC for each recycled stream can be attributed to the higher production of hydroxysodalite. Moreover, higher concentration of metallic ions can hamper the production of zeolite-A, therefore, consecutive recycling of the waste stream can reduce the CEC of the product.

Acknowledgment

The authors gratefully acknowledge the Natural Sciences and Engineering Council of Canada (NSERC) and Newalta.

Author's Contributions

The experiments were conducted by Dr. Salman Bukhari as part of his PhD research project, under the supervision of Prof. Sohrab Rohani. The draft of the manuscript was prepared by Salman Bukhari and revised by Sohrab Rohani.

Ethics

The material presented in this manuscript are the work of the authors.

References

- Aldahri, T., J. Behin, H. Kazemian and S. Rohani, 2016. Synthesis of zeolite Na-P from coal fly ash by thermo-sonochemical treatment. *Fuel*, 182: 494-501. DOI: 10.1016/j.fuel.2016.06.019
- Babajide, O., N. Musyoka, L. Petrik and F. Ameer, 2012. Novel zeolite Na-X synthesized from fly ash as a heterogeneous catalyst in biodiesel production. *Catal. Today*, 190: 54-60. DOI: 10.1016/j.cattod.2012.04.044
- Baerlocher, C., L.B. McCusker and D.H. Olson, 2007. *Atlas of Zeolite Framework Types*. 6th Edn., Elsevier, New York, ISBN-10: 0080554342, pp: 404.
- Bain, D.C. and B.F.L. Smith, 1987. *Chemical Analysis*. In: *Determinative Methods Clay Mater*, Blackie, Chapman and Hall, Glasgow, New York, pp: 248-274.
- Behin, J., S.S. Bukhari, H. Kazemian and S. Rohani, 2016. Developing a zero liquid discharge process for zeolitization of coal fly ash to synthetic NaP zeolite. *Fuel*, 171: 195-202. DOI: 10.1016/j.fuel.2015.12.073
- Behin, J., S.S. Bukhari, V. Dehnavi, H. Kazemian and S. Rohani, 2014. Using Coal Fly Ash and wastewater for microwave synthesis of LTA zeolite. *Chem. Eng. Technol.*, 37: 1532-1540. DOI: 10.1002/ceat.201400225

- Belviso, C., F. Cavalcante, A. Lettino and S. Fiore, 2009. Zeolite synthesised from fused coal fly ash at low temperature using seawater for crystallization. *Coal Combust. Gasif. Prod.*, 1: 7-13.
DOI: 10.4177/ccgp-d-09-00004.1
- Belviso, C., F. Cavalcante, A. Lettino and S. Fiore, 2011. Effects of ultrasonic treatment on zeolite synthesized from coal fly ash. *Ultrason. Sonochem.*, 18: 661-668. DOI: 10.1016/j.ultsonch.2010.08.011
- Breck, D.W., 1975. Zeolite molecular sieves: Structure, chemistry and use. *Anal. Chim. Acta*, 75: 493-493. DOI: 10.1016/S0003-2670(01)85391-5
- Bukhari, S.S., J. Behin, H. Kazemian and S. Rohani, 2014. A comparative study using direct hydrothermal and indirect fusion methods to produce zeolites from coal fly ash utilizing single-mode microwave energy. *J. Mater. Sci.*, 49: 8261-8271.
DOI: 10.1007/s10853-014-8535-2
- Bukhari, S.S., J. Behin, H. Kazemian and S. Rohani, 2015a. Conversion of coal fly ash to zeolite utilizing microwave and ultrasound energies: A review. *Fuel*, 140: 250-66. DOI: 10.1016/j.fuel.2014.09.077
- Bukhari, S.S., J. Behin, H. Kazemian and S. Rohani, 2015b. Synthesis of zeolite NA-A using single mode microwave irradiation at atmospheric pressure: The effect of microwave power. *Can. J. Chem. Eng.*, 93: 1081-1090. DOI: 10.1002/cjce.22194
- Bukhari, S.S., S. Rohani and H. Kazemian, 2016. Effect of ultrasound energy on the zeolitization of chemical extracts from fused coal fly ash. *Ultrason. Sonochem.*, 28: 47-53. DOI: 10.1016/j.ultsonch.2015.06.031
- Cheung, O. and N. Hedin, 2014. Zeolites and related sorbents with narrow pores for CO₂ separation from flue gas. *RSC Adv.*, 4: 14480-14494.
DOI: 10.1039/C3RA48052F
- Dehnavi, V., B.L. Luan, D.W. Shoesmith, X.Y. Liu and S. Rohani, 2013. Effect of duty cycle and applied current frequency on Plasma Electrolytic Oxidation (PEO) coating growth behavior. *Surf. Coat. Technol.*, 226: 100-107.
DOI: 10.1016/j.surfcoat.2013.03.041
- Derkowski, A., W. Franus, H. Waniak-Nowicka and A. Czimerova, 2007. Textural properties Vs. CEC and EGME retention of Na-X zeolite prepared from fly ash at room temperature. *Int. J. Miner. Process.*, 82: 57-68. DOI: 10.1016/j.minpro.2006.10.001
- Fan, Y., F.S. Zhang, J. Zhu and Z. Liu, 2008. Effective utilization of waste ash from MSW and coal co-combustion power plant-Zeolite synthesis. *J. Hazard. Mater.*, 153: 382-388.
DOI: 10.1016/j.jhazmat.2007.08.061
- Heidrich, C., H. Feuerborn and A. Weir, 2013. Coal combustion products: A global perspective. *World Coal Ash WOCA*, Lexington, KY.
- Holler, H. and U. Wirsching, 1985. Zeolite formation from fly ash. *Fortschr Mineral.*, 63: 21-43.
- Hollman, G.G., G. Steenbruggen and M. Janssen-Jurkovičová, 1999. A two-step process for the synthesis of zeolites from coal fly ash. *Fuel*, 78: 1225-1230. DOI: 10.1016/S0016-2361(99)00030-7
- Hussar, K., S. Teekasap and N. Somsuk, 2017. Synthesis of Zeolite a form by-product of aluminum etching process: Effects of reaction temperature and reaction time on pore volume. *Am. J. Environ. Sci.*, 7: 35-42. DOI: 10.3844/ajessp.2011.35.42
- IEA, 2013. *World energy outlook 2013*. International Energy Agency, Paris.
- Khan, A.Z., S. Nigar, S.K. Khalil, S. Wahab and A. Rab *et al.*, 2013. Influence of synthetic zeolite application on seed development profile of soybean grown on allophanic soil. *Pak. J. Bot.*, 45: 1063-1068.
- Khodabandeh, S., 1997. *Synthesis of alkaline-earth zeolites*. California Institute of Technology.
- Landau, M.V., L. Vradman, V. Valtchev, J. Lezervant and E. Liubich *et al.*, 2003. Hydrocracking of heavy vacuum gas oil with a Pt/H-beta-Al₂O₃ catalyst: Effect of zeolite crystal size in the nanoscale range. *Ind. Eng. Chem. Res.*, 42: 2773-2782.
DOI: 10.1021/ie020899o
- Malekpour, A., M.R. Millani and M. Kheirkhah, 2008. Synthesis and characterization of a NaA zeolite membrane and its applications for desalination of radioactive solutions. *Desalination*, 225: 199-208. DOI: 10.1016/j.desal.2007.02.096
- Moreno, N., X. Querol, C. Ayora, A. Alastuey and C. Fernández-Pereira *et al.*, 2001. Potential environmental applications of pure zeolitic material synthesized from fly ash. *J. Environ. Eng.*, 127: 994-1002.
DOI: 10.1061/(ASCE)0733-9372(2001)127:11(994)
- Moriyama, R., S. Takeda, M. Onozaki, Y. Katayama and K. Shiota *et al.*, 2005. Large-scale synthesis of artificial zeolite from coal fly ash with a small charge of alkaline solution. *Fuel*, 84: 1455-1461. DOI: 10.1016/j.fuel.2005.02.026
- Musyoka, N.M., L.F. Petrik and E. Hums, 2011. Ultrasonic assisted synthesis of zeolite A from coal fly ash using mine waters (acid mine drainage and circumneutral mine water) as a substitute for ultra pure water. *International Mine Water Association*, (MAW' 11), Aachen, Germany, pp: 423-428.
- Musyoka, N.M., L.F. Petrik, G. Balfour, W.M. Gitari and E. Hums, 2011. Synthesis of hydroxy sodalite from coal fly ash using waste industrial brine solution. *J. Environ. Sci. Health A*, 46: 1699-1707. DOI: 10.1080/10934529.2011.623961
- Musyoka, N.M., L.F. Petrik, O.O. Fatoba and E. Hums, 2013. Synthesis of zeolites from coal fly ash using mine waters. *Miner. Eng.*, 53: 9-15.
DOI: 10.1016/j.mineng.2013.06.019

- Querol, X., A. Alastuey, A. López-Soler, F. Plana and J.M. Andrés *et al.*, 1997. A fast method for recycling fly ash: Microwave-assisted zeolite synthesis. *Environ. Sci. Technol.*, 31: 2527-2533. DOI: 10.1021/es960937t
- Querol, X., J.C. Umaña, F. Plana, A. Alastuey and A. Lopez-Soler *et al.*, 2001. Synthesis of zeolites from fly ash at pilot plant scale. Examples of potential applications. *Fuel*, 80: 857-865. DOI: 10.1016/S0016-2361(00)00156-3
- Savage, N. and M.S. Diallo, 2005. Nanomaterials and water purification: Opportunities and challenges. *J. Nanoparticle Res.*, 7: 331-342. DOI: 10.1007/s11051-005-7523-5
- Shigemoto, N., H. Hayashi and K. Miyaura, 1993. Selective formation of Na-X zeolite from coal fly ash by fusion with sodium hydroxide prior to hydrothermal reaction. *J. Mater. Sci.*, 28: 4781-4786. DOI: 10.1007/BF00414272
- Shoumkova, A., 2011. Zeolites for water and wastewater treatment: An overview. Australian Institute of High Energy Materials.
- Sinha, P.K., P.K. Panicker, R.V. Amalraj and V. Krishnasamy, 1995. Treatment of radioactive liquid waste containing caesium by indigenously available synthetic zeolites: A comparative study. *Waste Manage.*, 15: 149-157. DOI: 10.1016/0956-053X(95)00014-Q
- Srinivasan, A. and M.W. Grutzeck, 1999. The adsorption of SO₂ by zeolites synthesized from fly ash. *Environ. Sci. Technol.*, 33: 1464-9146. DOI: 10.1021/es9802091
- Theron, J., J.A. Walker and T.E. Cloete, 2010. Nanotechnology and water treatment: Applications and emerging. *Nanotechnol. Water Treat. Applied*.
- Treacy, M.M.J. and J.B. Higgins, 2007. Collection of simulated XRD powder patterns for zeolites. Elsevier, Amsterdam, The Netherlands.
- Wang, S. and Y. Peng, 2010. Natural zeolites as effective adsorbents in water and wastewater treatment. *Chem. Eng. J.*, 156: 11-24. DOI: 10.1016/j.cej.2009.10.029
- Wang, S. and Z.H. Zhu, 2005. Sonochemical treatment of fly ash for dye removal from wastewater. *J. Hazard. Mater.*, 126: 91-95. DOI: 10.1016/j.jhazmat.2005.06.009
- Wdowin, M., M.M. Wiatros-Motyka, R. Panek, L.A. Stevens and W. Franus *et al.*, 2014. Experimental study of mercury removal from exhaust gases. *Fuel*, 128: 451-457. DOI: 10.1016/j.fuel.2014.03.041